

# High-Q and FOM Dual-Band Polarization Dependent Ultra-Narrowband Terahertz Metamaterial Sensor

E. Manikandan , K. A. Karthigeyan , A. Arivarasi, and E. Papanasam 

**Abstract**—Polarization-dependent dual-band THz metamaterial using a modified Trishul structure is proposed in this paper. The absorber has three layers namely, a conducting ground plane, a dielectric substrate, and a structure top metallic patch. The top and bottom metallic is made up of gold material and the dielectric substrate is polyimide. The characteristics are obtained using the finite element method. The structure has obtained two resonant peaks at 0.78 THz(f1) and 1.65 THz(f2) for the X-polarized wave and at 0.81 THz(f3) and 1.53 THz(f4) for the Y-polarized wave respectively. The simulation result reveals that the absorber has obtained ultra-narrow band absorption with a full width half maximum(FWHM) of 4.8 GHz, 10 GHz, 5 GHz, and 10 GHz for f1, f2, f3, and f4 respectively. In addition, the underlying physical mechanism of the multi-band characteristics is analyzed using electric field and surface current distributions. The proposed absorber design has importance in the emerging THz system for polarization imaging and sensing applications. Also, flexible metamaterials could be useful for soft robotics applications also.

**Index Terms**—Metamaterials, plasmonics, subwavelength structures, terahertz sensing.

## I. INTRODUCTION

IN RECENT years, sensors gained importance in a variety of applications including healthcare, environmental monitoring, the food industry, security applications, soft robotics, and so on. Sensors are used to gather the data and provide the necessary feedback to the system. These sensors improved the overall system performance and improved the lives of every individual in particular biosensors. Biosensors with proper signal conditioning circuits detect the biological signals and convert them into equivalent electrical output. According to the world health organization(WHO), cancer is a deadly disease that can happen in any part of the body organ, or tissue which further spreads out and leads to death. But early detection and identification of cancer disease may improve the mortality rate.

Manuscript received 13 November 2022; revised 19 December 2022; accepted 31 December 2022. Date of publication 13 January 2023; date of current version 20 January 2023. This work was supported by the Vellore Institute of Technology (VIT) management for open access. (*Corresponding author: E. Manikandan.*)

E. Manikandan is with the Centre for Innovation and Product Development, Vellore Institute of Technology – Chennai Campus, Chennai, Tamil Nadu 600127, India (e-mail: manikandan.e@vit.ac.in).

K. A. Karthigeyan is with the Department of Electronics and Communication Engineering, Vel Tech Rangarajan Dr. Sagunthala R&D Institute of Science and Technology, Chennai, Tamil Nadu 600062, India (e-mail: karthigeyanka.ssn@gmail.com).

A. Arivarasi and E. Papanasam are with the School of Electronics Engineering, Vellore Institute of Technology – Chennai Campus, Chennai, Tamil Nadu 600127, India (e-mail: arivarasi.a@vit.ac.in; papanasam.e@vit.ac.in).

Digital Object Identifier 10.1109/JPHOT.2023.3234074

The sensing of biological signals can be done in many ways. First, the electrochemical sensors in many methods such as amperometric, impedimetric, voltammetric, and potentiometric. The physical biosensor includes thermoelectric, piezoelectric, optical, and so forth. Each method has its advantages and drawbacks in terms of construction, cost, sensitivity, etc. In the optical method, the use of surface plasmon resonance (SPR) has gained more attention due to the following advantages: high accuracy, label-free detection, and low-volume sample requirement. The basic principle of this technique is refractive index sensing of the analyte. The changes in the refractive index are equivalently converted into transmission, reflection, and absorption characteristics. The change in the refractive index provides the shift in the resonance thereby the sensing can be done. This SPR usually arises when light interacts with the conducting electrons in the metals and nanostructures also exhibit this behavior [1], [2], [3].

At frequencies less than the visible region, it is possible to obtain spoof surface plasmon resonance by using metamaterials. Metamaterials are manmade periodic structures with a size less than the incident wavelength. Metamaterials have a special property negative index of refraction which is not available in natural materials. The geometry and material properties decide the resonant frequency of operation. Metamaterials find applications in sensing, imaging, modulation, soft robotics sensors, and so on. For the past two decades, the terahertz (THz) spectrum (0.1 to 10) THz has gained attraction in the field of research due to its unique characteristics such as non-ionizing, transparency to many plastics, biological fingerprints, etc. The developments of high-power laser sources such as quantum cascade laser, and HEMT structures made the researchers develop high-power THz sources and also detectors. In the literature, many aspects of developing high-power sources and detectors for THz radiation were introduced which led to the development of the components also [4]. Many variants of THz metamaterials were available in the literature and used for different applications.

The polarization-insensitive THz metamaterials were reported by many researchers and only a few focused on polarization-sensitive structures. But polarization-sensitive metamaterial is also helpful for polarization imaging and imaging applications. Polarization-sensitive metamaterial with better absorption characteristics in two orthogonal directions was designed and its analysis was reported [5]. The Cyclic olefin copolymer offers low loss in the THz frequencies and is being used as a dielectric substrate for components fabrication. A cross-shaped aperture-based frequency selective surface filter was designed and experimentally verified. This structure has

obtained polarization sensitivity with angle-resolved transmission characteristics for modulating applications. Also, the introduction of the substrate has produced guided mode resonances in addition to the fundamental resonance [6]. A polarization-controllable metamaterial was designed by using two horizontal and vertical metallic conducting strips. By adjusting the length of the strip, polarization-controllable absorption characteristics have been obtained. The structure has also obtained dual-band absorption behavior [7], [8]. These metamaterials are being used for sensing applications. The mechanism is that the changes in the refractive index change the resonant frequency of operation. This was applied for sensing biological signals. The metrics such as quality factor(Q-factor), Sensitivity, and Figure of Merit are deciding the characteristics of the sensor. Also, the increase in the number of publications could be seen from the obtained Scopus database which tells the curiosity of the researcher's interest in terahertz metamaterials. In addition to analyte sensing, temperature sensing was done by using a hexagonal resonator on an indium antimonide (InSb) substrate. The InSb substrate property helped in temperature sensing. It is also possible to obtain tunable metamaterial i.e., frequency reconfigurable by using materials like Graphene where the chemical potential decides the electrical conductivity. [9], [10], [11].

A single-band perfect absorber at a lower THz frequency was reported. The structure was a modified cylindrical resonator on a thin film polyimide substrate. But it was observed that the sensitivity was not improved even for the thicker analyte sample [12]. A narrowband absorber working at the visible region was reported and concluded that high Q-factor and FOM values were obtained due to narrowband absorption [13]. A highly sensitive dual-band sensor was designed with a sensitivity of around 100 GHz/RIU to 200 GHz/RIU using a circular ring resonator. The obtained FOM values were less than 1 and 5 at the first and second resonance respectively for the analyte thickness of 1  $\mu\text{m}$ . Further, the improvement in the sensitivity was obtained with asymmetric resonators [14], [15]. The simple circular resonator was designed and fabricated for sensing various citrate salts and experimentally verified using the THz-time domain spectroscopy method (THz-TDS). It was also noticed that metamaterial with band-stop characteristics could be used as a sensor. One such sensor was designed and the obtained sensitivity was very high compared to the earlier reported works. Still, the FOM values were less than 5 in the desired resonances. Also, different sensors using metamaterial were designed for sensing 4-Methylimidazole and virus variants have been reported [16], [17], [18], [19], [20]. From all these designs and analyses, it is observed that no polarization-sensitive multi-band sensor with High-Q and FOM is a need and to be explored.

In this research work, a polarization-sensitive dual-band terahertz metamaterial is designed and its analysis is carried out. The obtained four resonances individually help in sensing different analytes where these have a unique fingerprint. The sensing capability of the designed sensor is analyzed by varying the refractive index property and obtaining higher FOM values. Also, a detailed comparison with the literature is reported.

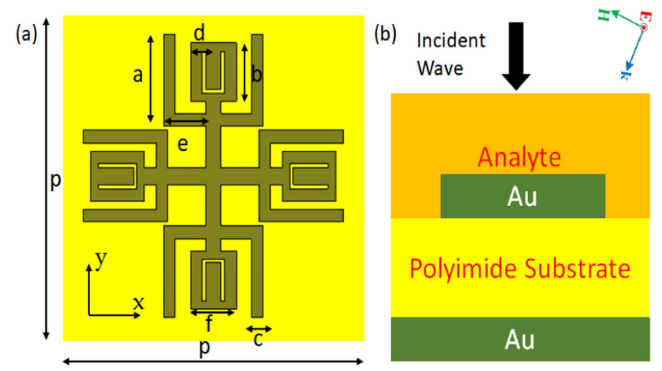


Fig. 1. (a) top view of the designed sensor with geometrical parameters (b) side view of the sensor with materials and incident wave direction.

TABLE I  
GEOMETRICAL PARAMETERS

Parameters	p	a	b	c	d	e	f
Value( $\mu\text{m}$ )	80	22	14	3	1	11	12

## II. PROPOSED DESIGN

The terahertz (THz) metamaterial sensor for sensing the analyte i.e., biomolecule, chemical components, etc. based on the refractive index property is designed and its analysis is carried out. The optimized structure of the proposed design is depicted in Fig. 1. The design is started with the four symmetrical resonators which usually give polarization-dependent characteristics. Then, the structure is modified and obtained as four Trishul structures with a cross aperture in the center. This helps in getting polarization-dependent multi-band characteristics. The overall design has three layers: the top and bottom metallic layers are separated by a polyimide dielectric substrate of thickness 2  $\mu\text{m}$ . The optimized geometrical parameters are listed in Table I.

## III. RESULTS AND DISCUSSIONS

### A. Absorption Characteristics

The numerical analysis of the designed unit cell is done using CST Microwave Studio software. The proposed sensor is analyzed using the Floquet mode theory which is being applied to analyzing the subwavelength elements. The periodic boundary conditions are used along the x and y directions with incident plane waves along the z-direction. For this simulation, a tetrahedral mesh is used for the computation with 10 cells per model and more than 15000 tetrahedrons. The minimum and maximum edge length are 0.1 m and 37 m respectively.

In general, the absorptivity  $A = 1 - T - R$  where A represents the absorption, T represents the transmission, and R represents the reflection. For the proposed design, beneath the polyimide substrate conducting ground plane is attached which usually reflects the incident thereby making zero transmission. Now the absorptivity becomes  $A = 1 - R$ . The designed structure has achieved near-zero reflection in the desired resonances thereby making near-unity absorption characteristics. The absorption

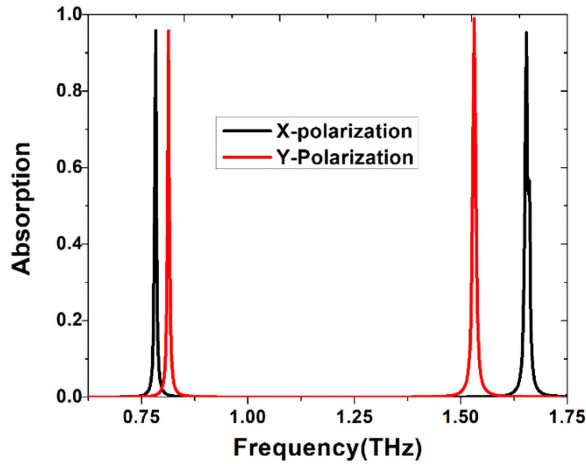


Fig. 2. Absorption characteristics of the designed structure for X and Y polarization.

characteristics of the designed structure for X and Y-polarization is shown in Fig. 2. The unity refractive index medium is used for all these analyses.

The structure has achieved polarization-sensitive dual-band absorption characteristics. The observed resonant frequencies are 0.78 THz( $f_1$ ) and 1.65 THz( $f_2$ ) for the X-polarized wave and 0.81 THz( $f_3$ ) and 1.53 THz( $f_4$ ) for the Y-polarized wave respectively. In total, the structure has obtained four resonances. Based on the biomolecule fingerprint the particular resonance is selected for improving the sensitivity of detection. The structure has also obtained an ultra-narrowband absorption i.e., FWHM of 4.8 GHz, 10 GHz, 5 GHz, and 10 GHz for  $f_1$ ,  $f_2$ ,  $f_3$ , and  $f_4$  respectively. This narrowband behavior helped in increasing the Q-factor which further affects the figure of merit characteristics of the sensor.

The proposed absorber has achieved near unity absorption i.e., more than 96.5% in all resonances. In particular, at 1.53 THz it is observed that 99% of absorption of the incident wave takes place.

The designed structure is tested for different polarization angles varying from  $0^\circ$  to  $60^\circ$  in an incremental order of  $15^\circ$  and the results are shown in Fig. 3(a) and (b) for X and Y-polarization respectively. It is clearly evident that the structure supports angle-resolved absorption characteristics for both the X and Y-polarized waves. This characteristic helps further for polarization imaging applications.

### B. Surface Plasmon

For understanding the physical phenomena of dual-band and spoof surface plasmon resonance characteristics of the proposed design, the electric and magnetic fields ( $E$  &  $H$  field) along the  $z$ -direction and the surface current distributions for the four resonances are obtained. First, will consider the case of X-polarization. The first resonance peak ( $f_1$ )  $E_z$ ,  $H_z$ , and the corresponding surface current distribution are shown in Figs. 4(a), 5(a), and 6(a) respectively. These distributions reveal that the vertical structure is responsible for the resonance. From the  $E_z$

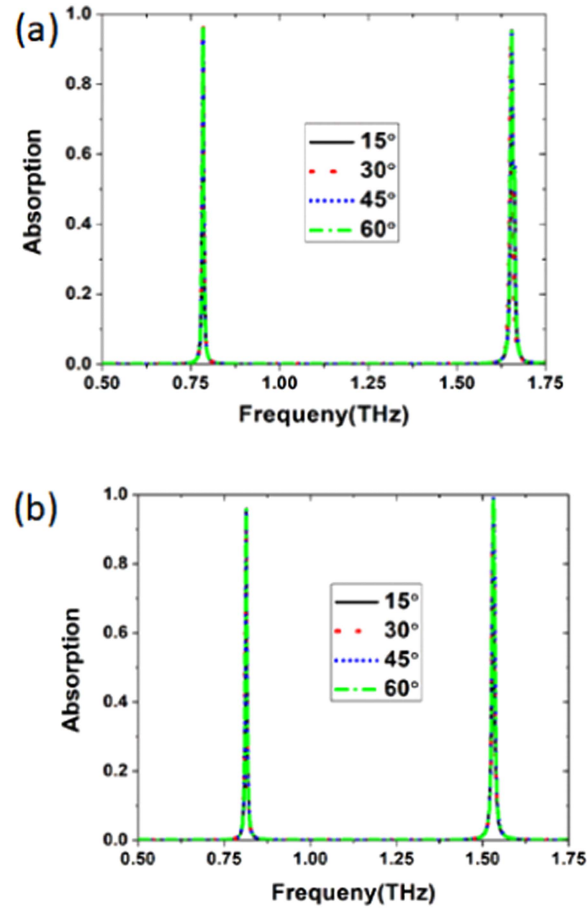


Fig. 3. Absorption characteristics of the designed structure for different polarization angles (a) X-polarized wave and (b) Y-polarized wave.

distributions, it is also observed that the opposite charge carriers are collected at each end of the vertical strip. From the  $H_z$  distribution, it is observed that a magnetic dipole is formed between the horizontal slots. This also confirms Huygens' principle [21]. In a similar way, the charge carriers for  $E_z$  are gathered at each end of the horizontal strip for the resonance  $f_2$ . The  $E_z$ ,  $H_z$ , and surface current distribution are shown in Figs. 4(b), 5(b), and 6(b) respectively. Now consider the second case Y-polarization. In a similar fashion to X-polarization, the horizontal and vertical strips are now responsible for  $f_3$  and  $f_4$  peaks. The  $E_z$ ,  $H_z$  and surface current distributions are depicted in Figs. 4(c), (d), 5(c), (d), and 6(c), (d) respectively for the resonances  $f_3$  and  $f_4$ . But the important observation in the  $E_z$  distributions is the entire structure is responsible for these two resonances with the respective strip dominating the mechanism.

### C. Sensing Characteristics

The sensing capability of the designed structure is evaluated by varying the refractive index of the analyte from 1 to 2.45. For the normal and affected cells for example in the case of cancer, the refractive index will be changing. So refractive index sensor is used for these applications. The thickness of the analyte is kept constant at  $1 \mu\text{m}$  throughout the analysis purpose. The

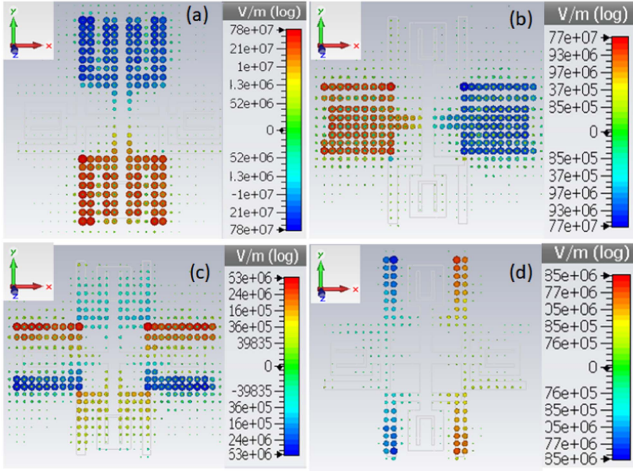


Fig. 4. E-field distribution along the z-direction at the surface of the designed metamaterial absorber (a) f1 (b) f2 (c) f3 (d) f4.

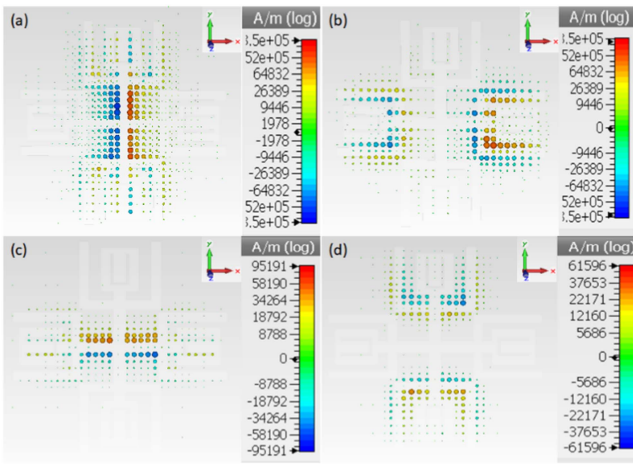


Fig. 5. H-field distribution along the z-direction at the surface of the designed metamaterial absorber (a) f1 (b) f2 (c) f3 (d) f4.

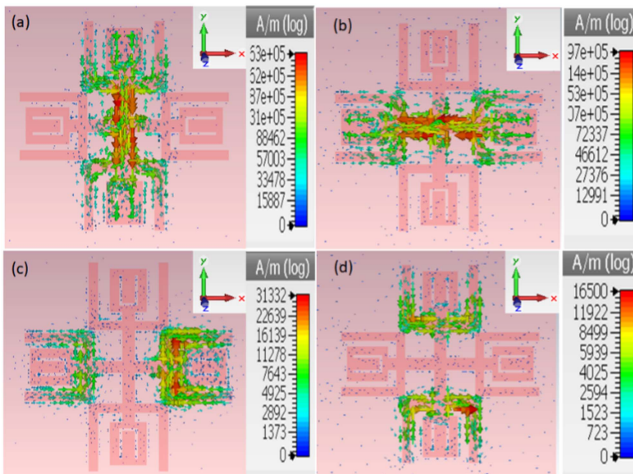


Fig. 6. Current distributions through the top surface of the designed metamaterial absorber at (a) f1 (b) f2 (c) f3 (d) f4.

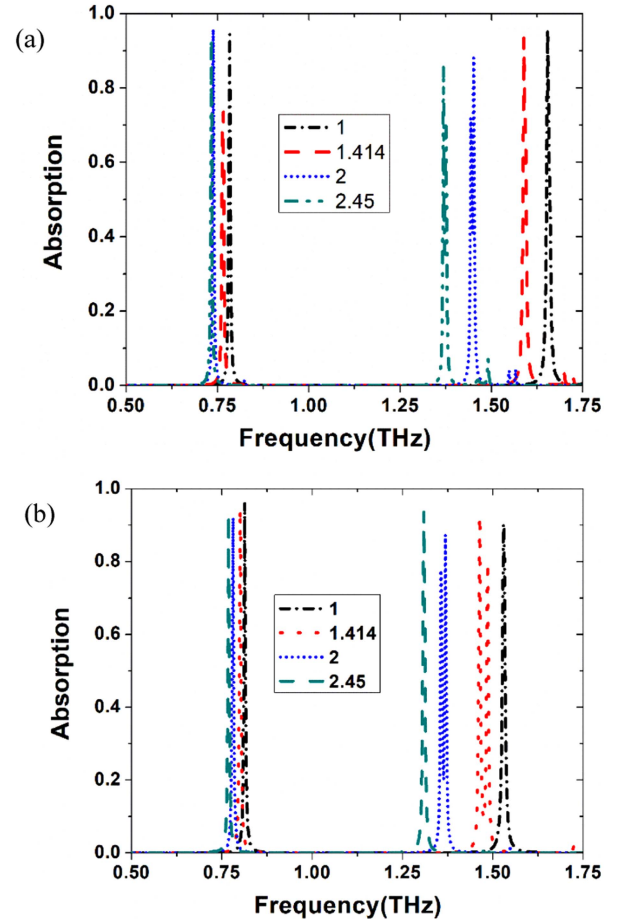


Fig. 7. Absorption characteristics of the designed sensor for incident analyte refractive index from 1 to 2.45 (a) X-polarization (b) Y-Polarization.

reason is to understand the applicability of the designed sensor for detecting the lower limit value. For the analyte thickness below  $0.5 \mu\text{m}$ , the shift in resonances is not appreciable. So the minimum thickness is kept at  $1 \mu\text{m}$ .

The obtained absorption characteristics of the designed sensor for incident analyte refractive index for X and Y polarization are shown in Fig. 7(a) and (b) respectively. Initially, the refractive index varied from 1 to 1.414 the red shift in frequency is observed in all resonances. The shift in resonance concerning the incident analyte is shown in Fig. 8(a) and (b) for X and Y-polarization respectively.

The ability of the designed sensor for application is decided by the following metrics. The Q-factor, Sensitivity, and figure of merit (FOM) are calculated as follows. The Q-factor is defined as the ratio of resonant frequency to the FWHM of the resonance. And,

$$\text{Sensitivity, } S = \Delta f / \Delta n, \quad (1)$$

Where  $\Delta f$  represents the shift in resonance and  $\Delta n$  is the change in refractive index and

$$\text{FOM} = S / \text{FWHM} \quad (2)$$

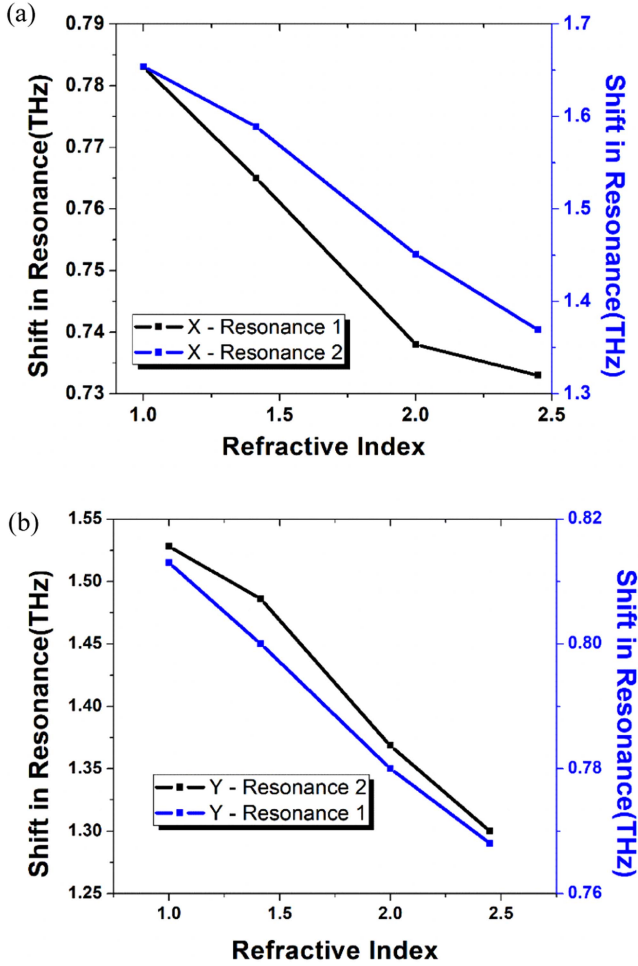


Fig. 8. Shift in the resonance with respect to the incident analyte refractive index (a) X-polarization (b) Y-Polarization.

At the resonance f1, the FWHM is only 4.8 GHz which indicates the ultra-narrowband operation of the sensor. Similarly, in the remaining resonances also, a max FWHM of 10 GHz is obtained. These FWHM values made the sensor achieve high Q-factor values i.e., more than 150 in all the resonances. The sensitivity looks normal values comparable to the reported works but, these obtained a higher value of FOM in all four resonances. The obtained metrics of the designed sensor for the four resonances are projected in Table II. It is also observed and impressed that the structure has obtained higher sensitivity and FOM value at f2 and f4 resonance. The salient feature of the proposed design is an easy fabrication which requires only surface-level etching. The feature size is also in the order of  $\mu\text{m}$  which can be fabricated by using basic chemical etching or ultrashort laser machining technique. This makes the design more useful for real-time sensing applications.

#### IV. FEATURES OF THIS WORK

The comparative analysis with the existing works is reported in Table III. On comparing, the designed sensor has the following distinct features 1) reporting high Q-factor resonances due to

TABLE II  
METRICS OF THE DESIGNED METAMATERIAL SENSOR

Resonance	*PA (%)	Q-Factor	S (GHz/RIU)	FWHM (GHz)	FOM (RIU <sup>-1</sup> )
f1	96.5	162.5	34.5	4.8	7.2
f2	99	165	196.5	10	19.65
f3	96.5	162.4	31	5	6.2
f4	96.5	152	157.25	10	15.725

PA-Peak Absorption (without analyte)

TABLE III  
A COMPARATIVE STUDY OF THE PROPOSED SENSOR WITH THE LITERATURE IN TERMS OF Q-FACTOR, S AND FOM

Ref	Frequency (THz)	Q-Factor	S (GHz/RIU)	FOM (RIU <sup>-1</sup> )
[10]	0.4	66.7	-	-
[12]	0.54, 2.01	4.54, 40.2	99, 242	0.67, 37
[15]	0.97, 2.88	7.65, 7.87	188, 573	1.53, 1.57
[17]	2.249	22.05	300	2.94
[18]	1.021, 1.52	26.2, 25.8	100, 168	2.56, 2.85
Proposed sensor	0.78, 0.81, 1.53, 1.65	162.5, 162.4, 152, 165	34.5, 31, 157.25, 196.5	7.2, 6.2, 15.725, 19.65

ultra-narrowband absorption 2) Higher FOM values for the four resonances 3) higher sensitivity in the higher order resonances 4) very simple structure and easy to fabricate. With these salient features, the designed sensor has achieved better metrics compared to the earlier reported work.

#### V. CONCLUSION

In summary, a novel dual-band polarization-dependent terahertz metamaterial absorber is designed and its numerical analysis is carried out using the FEM method. The design has obtained ultra-narrowband absorption in the desired resonances with angle-independent absorption characteristics. The sensing characteristics of the proposed design are evaluated numerically with a refractive index of the analyte varying from 1 to 2.5. The design has achieved a high Q-factor of 162.5, 165, 162.4, and 152 for f1, f2, f3, and f4 respectively with a corresponding sensitivity of 34.5 GHz/RIU, 196.5 GHz/RIU, 31 GHz/RIU

and 157.25 GHz/RIU. The major advantage observed in the design is it has achieved a high FOM of  $7.2\text{RIU}^{-1}$ ,  $19.65\text{RIU}^{-1}$ ,  $6.2\text{RIU}^{-1}$ , and  $15.725\text{RIU}^{-1}$  for the four resonances.

#### REFERENCES

- [1] B. P. Crulhas, C. R. Basso, G. R. Castro, and V. A. Pedrosa, "Review—Recent advances based on a sensor for cancer biomarker detection," *ECS J. Solid State Sci. Technol.*, vol. 10, 2021, Art. no. 047004.
- [2] T. Wang, A. Ramnarayanan, and H. Cheng, "Real time analysis of bioanalytes in healthcare, food, zoology and botany," *Sensors*, vol. 18, pp. 1–27, 2018.
- [3] A. Ahmadvand and B. Gerislioglu, "Photonic and plasmonic metasensors," *Laser Photon. Rev.*, vol. 16, 2022, Art. no. 2100328.
- [4] E. Manikandan, S. S. Princy, B. S. Sreeja, and S. Radha, "Structure metallic surface for terahertz plasmonics," *Plasmonics*, vol. 14, pp. 1311–1319, 2019.
- [5] F. Hu et al., "Polarization-dependent terahertz metamaterial absorber with high absorption in two orthogonal directions," *Opt. Commun.*, vol. 332, pp. 321–326, 2014.
- [6] A. Ferraro, D. C. Zografopoulos, R. Caputo, and R. Beccherelli, "Angle-resolved and polarization-dependent investigation of cross-shaped frequency-selective surface terahertz filters," *Appl. Phys. Lett.*, vol. 110, 2017, Art. no. 141107.
- [7] B. X. Wang et al., "Design of dual-band polarization controllable metamaterial absorber at terahertz frequency," *Results Phys.*, vol. 17, 2020, Art. no. 103077.
- [8] S. Quader, S. Quader, M. R. Akram, F. Xiao, and W. Zhu, "Graphene based ultra-broadband terahertz metamaterial absorber with dual-band tenability," *J. Opt.*, vol. 22, 2020, Art. no. 095104.
- [9] T. Parvin, K. Ahmed, A. M. Alatwi, and A. N. Z. Rashed, "Differential optical absorption spectroscopy-based refractive index sensor for cancer cell detection," *Opt. Rev.*, vol. 28, pp. 134–143, 2021.
- [10] B. Appasani, "A hybrid terahertz metamaterial sensor using a hexagonal ring resonator with bio-medical applications," *Plasmonics*, vol. 17, pp. 519–524, 2022.
- [11] F. Lotfi, N. Sang-Nourpour, and R. Kheradmand, "All-optical tunable plasmonic biosensor made of graphene and metamaterial," *Plasmonics*, vol. 17, pp. 799–809, 2022.
- [12] A. Elakkiya, S. Radha, B. S. Sreeja, and E. Manikandan, "Terahertz metamaterial absorber with sensing capabilities," *J. Optoelectron. Adv. Mater.*, vol. 22, pp. 360–364, 2020.
- [13] M. Pan et al., "A narrowband perfect absorber with high Q-factor and its application in sensing in the visible region," *Results Phys.*, vol. 19, 2020, Art. no. 103415.
- [14] X. He et al., "High-sensitive dual-band sensor based on microsize circular ring complementary terahertz metamaterial," *J. Electromagn. Waves Appl.*, vol. 31, pp. 91–100, 2017.
- [15] Z. Liu et al., "High-Q metamaterials based on cavity mode resonance for THz sensing applications," *AIP Adv.*, vol. 10, 2020, Art. no. 075014.
- [16] X. Deng et al., "Terahertz metamaterial sensor for sensitive detection of citrate salt solutions," *Biosensors*, vol. 12, 2022, Art. no. 408.
- [17] X. Lu, H. Ge, and Y. A. Jiang, "Dual-band high-sensitivity THz metamaterial sensor based on split metal stacking ring," *Biosensors*, vol. 12, no. 7, 2022, Art. no. 471.
- [18] H. J. Shin, H. W. Jang, and G. Ok, "Highly sensitive detection of 4-methylimidazole using a terahertz metamaterial," *Sensors*, vol. 18, 2018, Art. no. 4304.
- [19] A. S. Saadeldin, M. F. O. Hameed, E. M. A. Elkaramany, and S. S. A. Obayya, "Highly sensitive terahertz metamaterial sensor," *IEEE Sensors J.*, vol. 19, no. 18, pp. 7993–7999, Sep. 2019.
- [20] A. Kovačević, M. Potrebić, and D. Tošić, "Sensitivity characterization of multi-band THz metamaterial sensor for possible virus detection," *Electron.*, vol. 11, 2022, Art. no. 699.
- [21] M. R. Akram, C. He, and W. Zhu, "Bi-layer metasurface based on Huygens' principle for high gain antenna applications," *Opt. Exp.*, vol. 28, pp. 15844–15854, 2020.